

STRUCTURAL AND MAGNETIC CHARACTERIZATIONS OF BARIUM-STRONTIUM-FERRITES USING HEMATITE OF ANALYTICAL GRADE AND MAGNETITE FROM COX'S BAZAR BEACH SAND MINERAL

Ummay HABIBA¹, Hasan Khaled ROUF^{1*}, Sheikh Manjura HOQUE²

¹Department of Electrical and Electronic Engineering, University of Chittagong, Chittagong – 4331, Bangladesh

²Material Science Division, Bangladesh Atomic Energy Centre, Ramna, Dhaka, Bangladesh

Abstract

This article presents the characterizations of $BaO.SrO.xFe_2O_3$ and $BaO.SrO.xFe_3O_4$ ($x= 5.6, 5.8, 6$) hexaferrites. We have used hematite of analytical grade and magnetite from Cox's Bazar beach sand mineral to prepare these samples. Structural characteristics of the compositions have been revealed by the Scanning Electron Microscopic (SEM) tests. Magnetic characterizations have been performed by the Vibrating Sample Magnetometer (VSM) test and Mossbauer spectroscopy. From VSM test, we have determined the hysteresis parameters of the samples. The Curie temperatures of those hexaferrites have been obtained from the temperature dependent magnetic moments. The Mossbauer study indicates that the samples are in the ferromagnetic state and they are hexagonal ferrites.

Keywords: hexaferrite, magnetism, curie temperature, ferromagnet, hardmagnet.

Introduction

With the rapid development of technology, there is an increasing demand for various permanent magnets. Magnetic materials include a wide variety of materials, which are used in versatile range of applications. Ferrite materials dominate over other magnetic materials due to their low cost, high stability and versatile applications in the development of the current technology [1]. Ferrites are generally obtained from wide range of minerals and synthetic materials, and they have been used in different fields of interests for a long time [2]. M-type hexaferrites containing the Me ions have been widely used as permanent magnet. The ferromagnetic oxides with hexagonal crystal structure are called hexagonal ferrites [3]. The general formula for representing hexagonal ferrites is $m(MeO).n(Fe_2O_3)$, where Me = Ba, Sr, or Pb. The two formula units of $MeFe_{12}O_{19}$ per unit cell and the Fe^{+3} ions distributed over five non-equivalent crystallographic positions are responsible for building blocks of hexagonal crystal [4].

Hexagonal ferrites exhibit a hard and brittle magnetic behavior, which includes high coercive field, and high permeability in one plane and low permeability in other directions. These result in their high reactivity and subsequently low temperature processing to produce a better material in terms of activity parameters [5]. Although barium ferrite is the most common hexaferrite, nowadays strontium ferrites have become an excellent supplement to the former owing to its higher coercive force [6].

In recent years, there have been many works on the synthesis and characterization of hexagonal ferrites. The influence of the admixture of group III elements upon magnetic

properties of the Ba-Sr-ferrite has been investigated by Wlodzimierz [7]. Admixture of B_2O_3 did not favour the synthesis. For low concentration of B_2O_3 a slight increase in saturation magnetization was found while for high concentration of B_2O_3 the saturation magnetization was decreased. Nanocrystalline particles of barium hexaferrite were synthesized by a sol-gel combustion route in [8]. The effect of addition of polyethylene glycol (PEG) solutions with different molecular weights on magneto-structural properties of barium hexaferrite was also studied there. In [4] strontium hexaferrite nanoparticles had been prepared by co-precipitation in aqueous solutions and precipitation in microemulsion system water/SDS/n-butanol/ cyclohexane. Iron and strontium nitrates in different molar ratios were used as the starting materials. The precursors of nanocrystalline particles of $SrFe_{12}O_{19}$ with average particle size of around 30 nm and relatively high specific magnetization were successfully prepared. In [9] strontium hexaferrite ($SrFe_{12}O_{19}$ -SrF) powders have been prepared by the sol-gel process and magnetic properties of conventional and microwave calcined strontium hexaferrite powders have been studied. The advantages and disadvantages of Ba and Sr ferrite magnets as well as applications of ferrites in high-efficiency motors are discussed in [6]. Reference [10] investigated the magnetic and structural properties of copper substituted Barium ferrite powder particles via co-precipitation method. Copper-doped barium ferrite increases the coercivity and the magnetic storage capacity of the permanent magnet. In this work, Barium-Strontium-Ferrites have been prepared using Hematite of Analytical Grade and Magnetite from Cox's Bazar Beach Sand Mineralsto characterize their structural and magnetic properties for permanent magnet applications. $BaO.SrO.xFe_2O_3$ and $BaO.SrO.xFe_3O_4$ ($x=5.6, 5.8, 6$) samples have been prepared by solid-state method. These Barium-Strontium-Ferrites were prepared using the same procedure as described in [11]. In [11] the X-ray diffraction measurement was performed to reveal their structural properties. In our present study, we have performed the Scanning Electron Microscopy (SEM) to determine the structural properties of those samples. Mossbauer spectroscopy as well as magnetic hysteresis measurements and temperature dependence of permeability measurements have been performed to determine magnetic properties.

Experimental Details

Sample preparation

Sample preparation technique is an important part for ferrites processing. The usual method of preparing ferrite comprises of conventional ceramic method i.e. solid state reaction method involving milling of reactions followed by sintering. To synthesize the sample we followed this method. $BaCO_3$, $SrCO_3$ and hematite were used to prepare $BaO.SrO.xFe_2O_3$ ($x=5.6, 5.8, 6$) while $BaCO_3$, $SrCO_3$ and magnetite were used to prepare $BaO.SrO.xFe_3O_4$ ($x=5.6, 5.8, 6$). Intimate mixing of the materials was carried out using agate mortar (hand milled) for 4 hours for fine homogeneous mixing. Then the mixed samples were pre-sintered at a temperature between $850^{\circ}C$ to $900^{\circ}C$ for 5 hours to form ferrite through chemical reaction. The pre-sintered materials were milled for another 4 hours in distilled water to reduce them to small crystallites of uniform size. The mixtures were then dried and a small amount of saturated solution of polyvinyl alcohol was added as a binder. The resulting powder were pressed uniaxially under a pressure of $15-20 KN.cm^{-2}$ in a stainless steel die to make pellets, rods and toroids. Then the pressed pellet, rod and toroid shaped samples were finally sintered at $1250^{\circ}C$ temperature for 4 hours and then cooled in the furnace. The XRD patterns confirmed that the samples were phase pure. Small

pieces were cut from the sintered pellets with weight 0.005– 0.01 g for different characterizations.

Physiochemical characterization

The ferrite materials were characterized to evaluate their compositional and magnetic properties. We used Scanning Electron Microscopy (SEM) to determine the grain size of the materials and to compare the size with the change of compositions of the ferrite contents. The hysteresis loop has been measured for each sample using Vibrating Sample Magnetometer (VSM). From the VSM tests, we have also obtained the saturation magnetization, remanent magnetization and coercive field of the samples. The saturation magnetization is the maximum value after which the magnetization remains constant with the increase of the magnetic field. And the remanent magnetization is the magnetization which is obtained when the applied magnetic field is zero. The coercive field is the applied external field responsible for obtaining zero magnetization. The Curie temperature for each sample has been determined by moment vs. temperature (M-T) curves and dM/dT vs. T curves. Mossbauer analysis was performed to observe the Mossbauer spectra and to determine the magnetic hyperfine field, the isomer shift and the electrical quadrupole splitting and for each sample.

Results and Discussions

Scanning Electron Microscopy (SEM)

We used scanning electron microscopic (SEM) tests to determine the structural characteristics of the composition. The grain-size of the materials were determined and shown in Fig. 1 and Table 1.

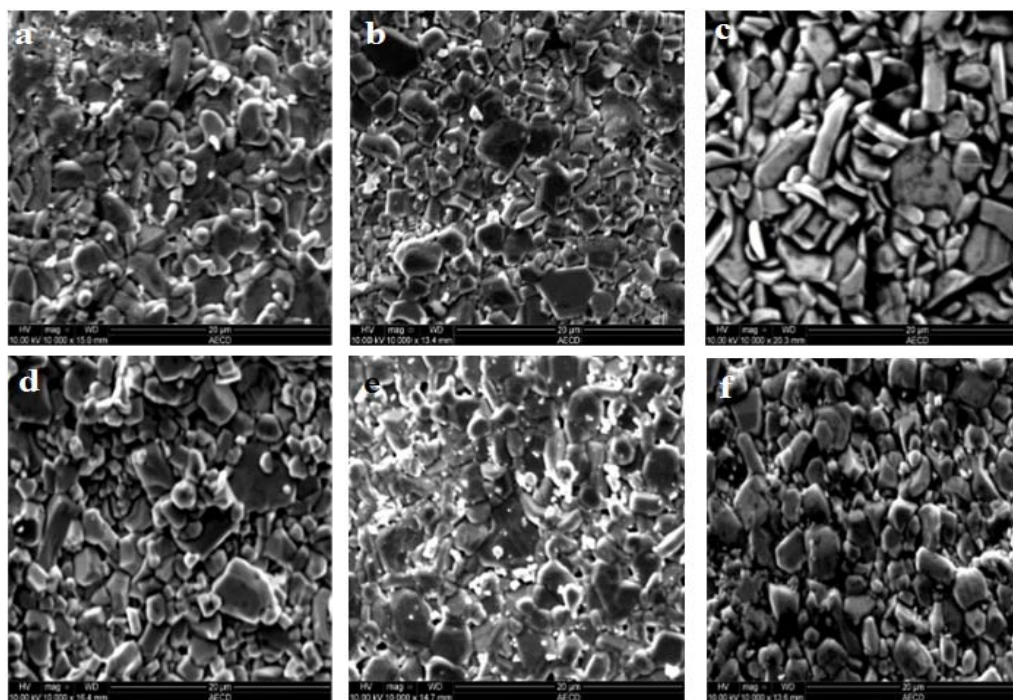


Fig.1. Grain size of $BaO.SrO.xFe_2O_3$ for (a) $x=5.6$, (b) $x=5.8$, (c) $x=6$ and $BaO.SrO.xFe_2O_4$ for (d) $x=5.6$, (e) $x=5.8$, (f) $x=6$.

Grain-sizes of both $\text{BaO.SrO.xFe}_2\text{O}_3$ and $\text{BaO.SrO.xFe}_3\text{O}_4$ for different values of x are shown. Both Fig. 1 and Table 1 show that the average grain size depends on the value of x . With the increase of x , the average grain size also increases. Fig. 2 graphically shows how the grain-size is changed with the values of x . Here the average grain sizes are plotted against the concentration of the ferrite elements. We observe that the average grain size of the $\text{BaO.SrO.xFe}_2\text{O}_3$ is greater than that of the $\text{BaO.SrO.xFe}_3\text{O}_4$.

Table 1. Average grain sizes of the samples

| | Grain size (μm) for $x=5.6$ | Grain size (μm) for $x=5.8$ | Grain size (μm) for $x=6$ |
|-------------------------|--|--|--|
| Fe_2O_3 | 1.94 | 2.5 | 3.7 |
| Fe_3O_4 | 1.73073 | 2.0046 | 2.11407 |

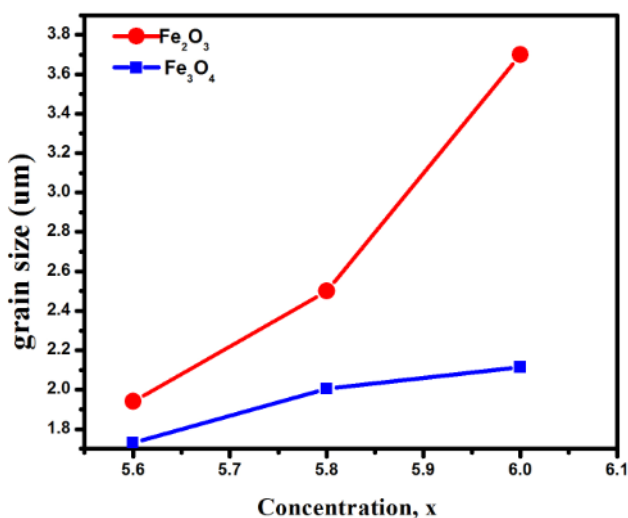


Fig.2. Change of grain size of the materials with x .

Vibrating Sample Magnetometer (VSM)

The hysteresis parameters of the compositions have been studied by Vibrating Sample Magnetometer (VSM) tests. Fig. 3 shows the hysteresis loops for Ba-Sr-ferrites using hematite and magnetite. The hysteresis loops indicate that the samples are of ferromagnetic type. Next we studied the temperature dependence of magnetic moments of $\text{BaO.SrO.xFe}_2\text{O}_3$ and $\text{BaO.SrO.xFe}_3\text{O}_4$. Fig. 4 shows the magnetic moment vs. temperature (M-T) curves for all of the compositions. The Curie temperatures of different compositions can be obtained from such study. We also observed the dM/dT versus T curve as shown in Fig. 5. All the magnetic parameters obtained from the VSM tests are summarized in Table 2.

The coercive fields, remanent magnetizations (M_r), saturation magnetization (M_s) and Curie temperature (T_c) for different values of x are shown in Table 2. All the samples have very high coercive fields, remanent magnetizations (M_r), saturation magnetization (M_s) and Curie temperature (T_c) which further confirms their strong ferromagnetic nature. We observe that the saturation magnetization of both Ba-Sr-ferrites decreases with the decreasing values of x . The

coercive fields for the samples using hematite (Fe_2O_3) are higher than that for the samples using magnetite (Fe_3O_4). Again the Curie temperatures for samples using hematite are higher than those of the samples using magnetite. All these results demonstrate that, the stability of magnetism is greater in $\text{BaO}.\text{SrO}.x\text{Fe}_2\text{O}_3$ than in $\text{BaO}.\text{SrO}.x\text{Fe}_3\text{O}_4$.

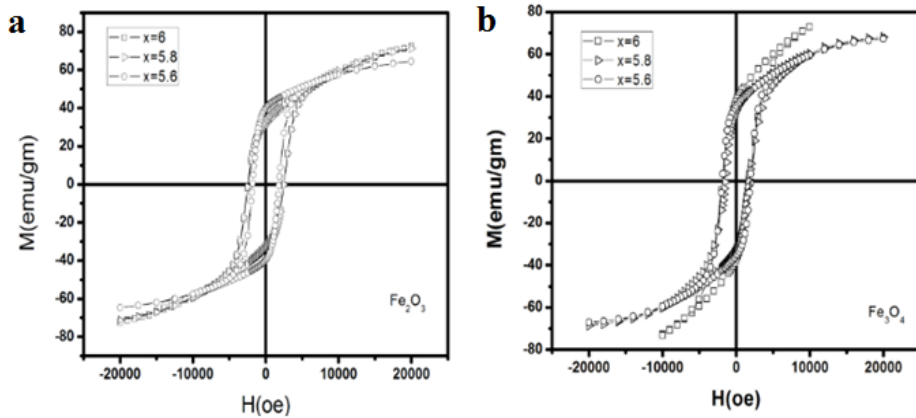


Fig.3. Hysteresis loop of Ba-Sr-ferrites (a) using Hematite and (b) using Magnetite.

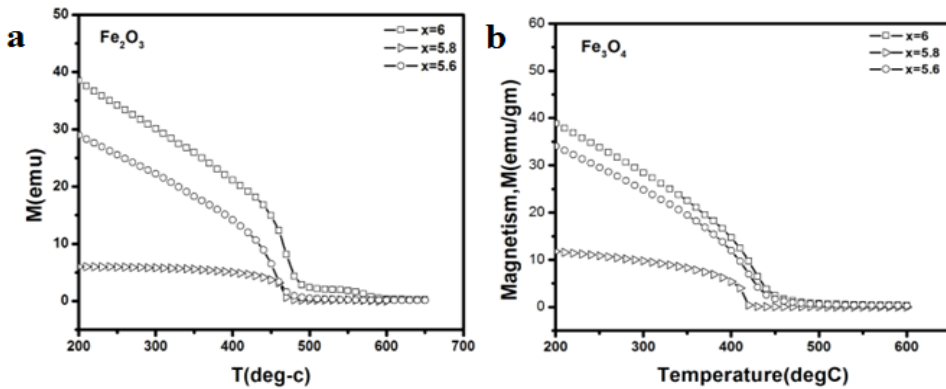


Fig. 4. M-T curves of Ba-Sr-ferrites (a) using Hematite and (b) using Magnetite.

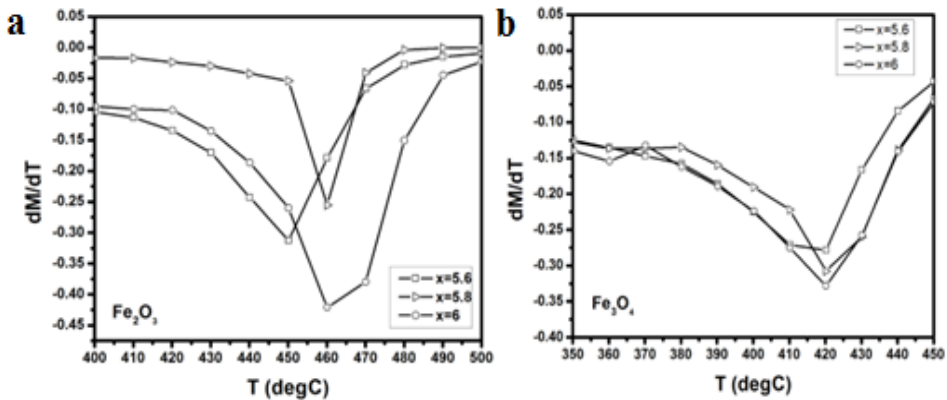


Fig.5. dM/dT versus T curves of Ba-Sr-ferrites (a) using Hematite and (b) using Magnetite.

Table 2. Magnetic parameters from VSM test

| x | Coercive field (oe) | Remanent magnetization, M_r (emu) | Saturation magnetization, M_s (emu) | $T_c(^{\circ}C)$ |
|-----------|---------------------|-------------------------------------|---------------------------------------|------------------|
| Fe_2O_3 | 6 | 2468.15 | 3.18E+01 | 460 |
| | 5.8 | 2476.096 | 3.35E+01 | 460 |
| | 5.6 | 1810.477 | 3.98E+01 | 450 |
| Fe_3O_4 | 6 | 1897.688 | 3.55E+01 | 420 |
| | 5.8 | 1931.297 | 3.76E+01 | 420 |
| | 5.6 | 1588.256 | 3.31E+01 | 420 |

Mossbauer spectroscopy

To estimate the distribution of iron (Fe^{3+}) in the ferrite, ^{57}Fe -Mossbauer spectra were recorded. Figure 6 shows the Mossbauer spectra for $BaO.SrO.xFe_2O_3$ and $BaO.SrO.xFe_3O_4$ ($x=5.6, 5.8 \& 6$). Both the theoretical data and fitted curves by least square method are shown in Fig. 6. Small circles indicates the theoretical data. The calculated spectrum of each individual component is represented by a continuous line. The hyperfine parameters of Mossbauer spectroscopy are shown in Table 3 and Table 4 for $BaO.SrO.xFe_2O_3$ and $BaO.SrO.xFe_3O_4$ respectively.

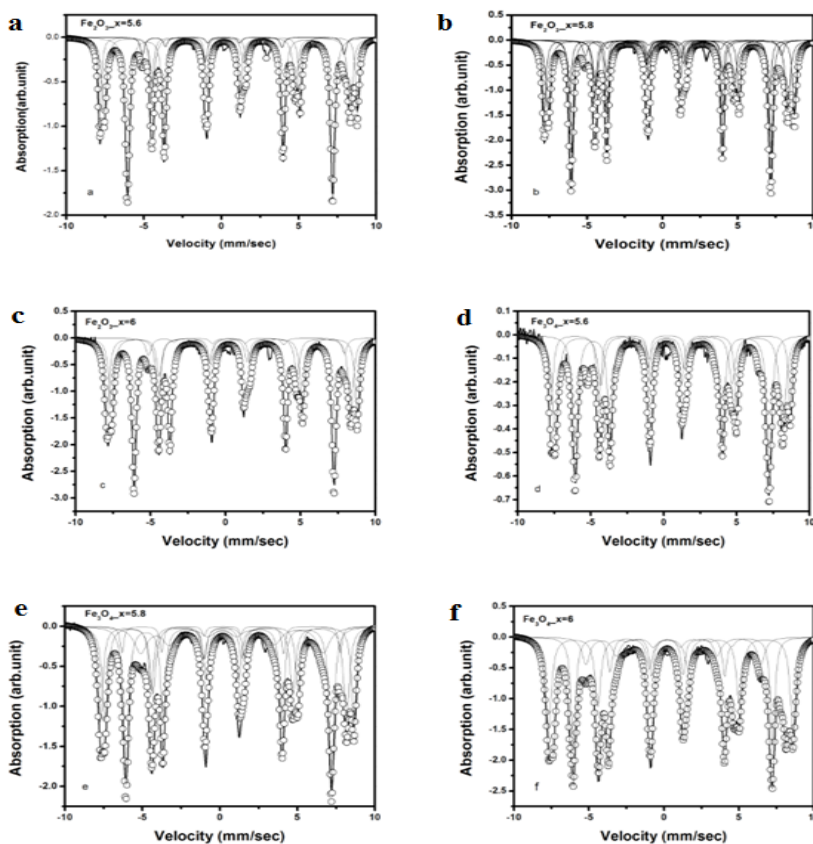


Fig. 6. Spectrum of Mossbauer Spectroscopy for $BaO.SrO.xFe_2O_3$ with (a) $x=5.6$, (b) $x=5.8$, (c) $x=6$ and $BaO.SrO.xFe_3O_4$ with (d) $x=5.6$, (e) $x=5.8$, (f) $x=6$. Circles (o) represent the theoretical data while the continuous lines correspond to least square fits.

Table 3. Hyperfine parameters for Samples using hematite

| Fe ₂ O ₃ | Sub-species | Chemical Shift (δ) mm/sec | Quadruple splitting (dEq) mm/sec | Hyperfine field (Hint) kG | Relative Area |
|--------------------------------|-------------|---------------------------------------|-------------------------------------|------------------------------|---------------|
| x=5.6 | Ia | 0.38 | 0.383 | -517.002 | 0.202 |
| | Ib | 0.354 | 0.414 | -412.295 | 0.497 |
| | II | 0.786 | 1.284 | -405.349 | 0.0482 |
| | IIIa | 0.201 | 0.966 | -337.461 | 0.0017 |
| | IIIb | 0.276 | 0.2 | -494.18 | 0.268 |
| x=5.8 | Ia | 0.376 | 0.18 | -516.877 | 0.225 |
| | Ib | 0.275 | 0.202 | -493.893 | 0.256 |
| | II | 0.752 | 1.302 | -404.71 | 0.0550 |
| | IIIa | 0.375 | 0.454 | -412.218 | 0.315 |
| | IIIb | 0.313 | 0.328 | -412.513 | 0.152 |
| x=6 | Ia | 0.155 | 1.25 | -424.731 | 0 |
| | Ib | 0.381 | 0.529 | -518.742 | 0.278 |
| | II | 0.805 | 1.5 | -402.103 | 0.0515 |
| | IIIa | 0.355 | 0.416 | -415.11 | 0.437 |
| | IIIb | 0.275 | 0.562 | -495.871 | 0.237 |

The mossbauer spectra of all the samples indicate that the samples are hexagonal ferrites consisting of 5 lattice sites. The Mossbauer spectra of those hexagonal samples are the results of superposition of spectra of those 5 sites for each sample. The line broadening of the spectrum increases with the increase of impurity in the sample. The broad spectra indicate the wide distribution of magnetic field on iron ions in the neighborhood of impurity atoms. The magnitude of the hyperfine field is a measure of the magnetic moment on the atoms in ferromagnetic alloys. The hyperfine magnetic field at the Iron nucleus is proportional to the magnetization of the sub-lattice [12-18].

Table 4. Hyperfine parameters for samples using magnetite

| Fe ₃ O ₄ | Sub-species | Chemical Shift (δ) mm/sec | Quadruple splitting (dEq) mm/sec | Hyperfine field (H _{int}) kG | RelativeArea |
|--------------------------------|-------------|---------------------------------------|-------------------------------------|--|--------------|
| x=5.6 | Ia | 0.102 | 0 | -400 | 0.0512 |
| | Ib | 0.376 | 0.512 | -509.518 | 0.196 |
| | II | 0.549 | 1.5 | -371.382 | 0.0706 |
| | IIIa | 0.374 | 0.424 | -414.093 | 0.404 |
| | IIIb | 0.273 | 0.411 | -484.635 | 0.308 |
| x=5.8 | Ia | 0.279 | 0.192 | -485.202 | 0.27 |
| | Ib | 0.382 | 0.161 | -509.425 | 0.235 |
| | II | 0.446 | 1.275 | -432.142 | 0.0574 |
| | IIIa | 0.455 | 0.637 | -366.926 | 0.16 |
| | IIIb | 0.367 | 0.439 | -412.806 | 0.369 |
| x=6 | Ia | 5.11e-18 | 2.50e-11 | -548.347 | 0.000 |
| | Ib | 0.381 | 0.308 | -507.379 | 0.278 |
| | II | 0.408 | 0.450 | -363.285 | 0.105 |
| | IIIa | 0.410 | 0.484 | -413.436 | 0.211 |
| | IIIb | 0.252 | 0.341 | -415.854 | 0.148 |

From the above hyperfine parameters, it is clear that those samples are ferromagnetic materials, because the hyperfine fields were obtained without applying any external magnetic field. The average hyperfine field of each ferrite increases with the increase of x . So the ferromagnetism of the materials increases with the values of x . Again the average HF field of $\text{BaO.SrO.xFe}_3\text{O}_4$ is larger than $\text{BaO.SrO.xFe}_2\text{O}_3$. So the ferromagnetism of $\text{BaO.SrO.xFe}_3\text{O}_4$ is higher than that of $\text{BaO.SrO.xFe}_2\text{O}_3$. The isomer shifts tend to be small, when HMFs usually provide large and distinct shifts of Mossbauer peak. They change with the valence of the iron ions. The quadrupole interaction is caused by an electric quadrupole moment in the atomic crystal lattice.

Conclusions

The structural as well as magnetic characterizations of $\text{BaO.SrO.xFe}_2\text{O}_3$ and $\text{BaO.SrO.xFe}_3\text{O}_4$ have been extensively studied in this work. Hematite from the analytical grades and magnetite from Cox's Bazar beach sand mineral have been used as ferrite elements. SEM tests showed that the average grain size is larger for $\text{BaO.SrO.xFe}_2\text{O}_3$ than that of $\text{BaO.SrO.xFe}_3\text{O}_4$. We also found that the grain size increases with the increase of x for both compositions. Studies of magnetic characterizations were performed by VSM tests and Mossbauer spectroscopy. The hysteresis loops indicate that all the samples are in ferromagnetic state. From the hysteresis parameters, we observed that the saturation magnetization increases with x for both of the compositions. $\text{BaO.SrO.xFe}_2\text{O}_3$ was found to have higher magnetic stability than $\text{BaO.SrO.xFe}_3\text{O}_4$ as the former has higher coercive field and higher Curie temperature. The Mossbauer spectra indicate that the ferrites are in hexagonal state. According to the hyperfine field of the samples, the ferromagnetism of the hexaferrites increases with the values of x and the ferromagnetism of $\text{BaO.SrO.xFe}_3\text{O}_4$ is higher than that of $\text{BaO.SrO.xFe}_2\text{O}_3$. We can say by correlating the results of both structural and magnetic characterizations that the magnetization is related to the grain size as well as concentration of ferrite contents and magnetization and magnetic stability increase with the grain size. But the smaller grain size is desirable to get smaller porosity. From the above results, we can conclude that, the hexaferrite materials using magnetite from the Cox's Bazar beach sand mineral are more suitable for ferromagnetic applications (for example, magnetic refrigeration) than the hexaferrites from hematite of analytical grade though the later has larger Curie temperature.

References

- [1] S.C. Mazumdar, A. K. M. A. Hossain, *Synthesis and Magnetic Properties of $\text{Ba}_2\text{Ni}_{2-x}\text{Zn}_x\text{Fe}_{12}\text{O}_{22}$ Hexaferrites*, **World Journal of Condensed Matter Physics**, **2**, 2012, pp. 181-187.
- [2] M.H. Yousefi, S. Manouchehri, A. Arab, M. Mozaffari, Gh. R. Amiri, J. Amighian, *Preparation of Cobalt-Zinc Ferrite ($\text{Co}_{0.8}\text{Zn}_{0.2}\text{Fe}_2\text{O}_4$) Nanopowder via Combustion method and Investigation of its Magnetic Properties*, **Materials Research Bulletin**, **45**, 2010, pp. 1792-1795.

- [3] G. Albanese, *Recent Advances In Hexagonal Ferrites By The Use Of Nuclear Spectroscopic Methods*, **Journal de Physique Colloques**, **38 (C1)**, 1977, pp. 85-94.
- [4] A Drmota, A Žnidaršič, A Košak, *Synthesis of Strontium Hexaferrite Nanoparticles Prepared using Co-precipitation Method and Microemulsion Processing*, **Journal of Physics**, **200**, 2010, pp. 1-4.
- [5] S. Kulkarni, J. Shrotri, C.E. Deshpande, S.K. Date, *Synthesis of Chemical Coprecipitated Hexagonal Strontium Ferrite and its Characterization*, **Journal of Materials Science**, **24**, 1989, pp. 3739-3744.
- [6] M.F. de Campos, D. Rodrigues, *High Technology Applications of Barium and Strontium Ferrite Magnets*, **Materials Science Forum**, **881**, 2016, pp 134-139.
- [7] W. Wolski, *Barium-Strontium Ferrite with Admixtures of Elements of the III-rd Group*, **Japanese Journal of Applied Physics**, **9**, 1070, pp. 711-715.
- [8] Z. Durmus, *A Comparative Study on Magnetostructural Properties of Barium Hexaferrite Powders Prepared by Polyethylene Glycol*, **Journal of Nanomaterials**, **2014**, 2014, pp. 1-7.
- [9] K. Samikannu, J. Sinnappan, S. Mannarswamy, T. Cinnasamy, K. Thirunavukarasu, *Synthesis and Magnetic Properties of Conventional and Microwave Calcined Strontium Hexaferrite Powder*, **Journal of Materials Sciences and Applications**, **2**, 2011, pp. 638-642.
- [10] S. Vadivelan, N. Victor Jaya, *Investigation of magnetic and structural properties of copper substituted barium ferrite powder particles via co-precipitation method*, **Journal of Results in Physics**, **6**, 2016, pp. 843–850.
- [11] S.M. Hoque, M.A. Hakim, D.K. Saha, *Synthesis and Characterization of Ba-Sr Hexaferrite Using Hematite of Analytical Grade and Magnetite from Cox's Bazar Beach Sand*, **Nuclear Science and Applications**, **15(1)**, 2006, pp. 65-70.
- [12] Y. Senzaki, J. Caruso, M. J. Hampden-Smith, Toivo T. Kodas, Lu-Min Wang, *Preparation of Strontium Ferrite Particles by Spray Pyrolysis*, **Journal of the American Ceramic Society**, **78**, 1995, pp. 2973-2976.
- [13] S. M. Ismail, Sh. Labib, S. S. Attallah, *Preparation and Characterization of Nano-Cadmium Ferrite*, **Journal of Ceramics**, **2013**, 2013, pp. 1-8.
- [14] H M Lu, W T Zheng, Q Jiang, *Saturation Magnetization Of Ferromagnetic And Ferrimagnetic Nanocrystals At Room Temperature*, **Journal of Physics D: Applied Physics**, **40**, 2007, pp. 320-325.
- [15] A.A. Kadir, A.S.A. Rahim, I.G. Sandu, M.M.A. Abdullah, A.V. Sandu, *Leachate Characteristic of Mosaic Sludge Brick*, **Revista de Chimie**, **67**, no. 5, 2016, pp. 978-983.
- [16] A.M. Mocanu, C. Luca, G. Ciobanu, S.I. Dunca, I.G. Sandu, A.C. Luca, *Synthesis, Characterization and Antimicrobial Activity of Some New Hydrazine Metallic Complexes*, **Revista de Chimie**, **66**, no. 8, 2015, pp. 1137-1142.
- [17] M. Nabialek, P. Pietrusiewicz, M. Szota, M.M.A. Abdullah, A.V. Sandu, *The Structure and Porosity of Fe_{62-x}Co₁₀WyMexY₈B_{20-y} Alloys in the Amorphous and Crystalline States (where: Me = Mo, Nb; x=0, 1, 2; y=0, 1, 2)*, **Revista de Chimie**, **68**, no. 1, 2017, pp.22-27.

- [18] M. Poiana, M. Dobromir, A.V. Sandu, V. Georgescu, *Investigation of Structural, Magnetic and Magnetotransport Properties of Electrodeposited Co-TiO₂ Nanocomposite Films*, **Journal Of Superconductivity And Novel Magnetism**, 25, 7, 2012, pp.2377-2387.
-

Received: March30, 2017

Accepted: September 15, 2017